Thermochimica Acta 502 (2010) 24–29

Contents lists available at ScienceDirect

Thermochimica Acta

journal homepage: www.elsevier.com/locate/tca

Thermal decomposition of potassium metaperiodate doped with trivalent ions

K. Muraleedharan*, M.P. Kannan, T. Gangadevi

Department of Chemistry, University of Calicut, Calicut, Kerala 673 635, India

ARTICLE INFO

Article history:
Received 25 September 2009
Received in revised form
14 December 2009
Accepted 26 January 2010
Available online 2 February 2010

Keywords:
Doping
Electron transfer
Isothermal decomposition
KIO_4
Kinetics and mechanism

ABSTRACT

The kinetics of isothermal decomposition of potassium metaperiodate (KIO_4), doped with phosphate and aluminium has been studied by thermogravimetry (TG). We introduced a custom-made thermobalance that is able to record weight decrease with time under pure isothermal conditions. The decomposition proceeds mainly through two stages: an acceleratory stages up to $\alpha = 0.50$ and the decay stage beyond. The decomposition data for aluminium and phosphate doped KIO_4 were found to be best described by the Prout–Tompkins equation. Separate kinetic analyses of the α–t data corresponding to the acceleratory region and decay region showed that the acceleratory stage gave the best fit with Prout–Tompkins equation itself whereas the decay stage fitted better to the contracting area equation. The rate of decomposition of phosphate doped KIO_4 increases approximately linearly with an increase in the dopant concentration. In the case of aluminium doped KIO_4, the rate passes through a maximum with increase in the dopant concentration. The α–t data of pure and doped KIO_4 were also subjected to isoconversional studies for the determination of activation energy values. Doping did not change the activation energy of the reaction. The results favour an electron-transfer mechanism for the isothermal decomposition of KIO_4, agreeing well with our earlier observations.

1. Introduction

The thermal decomposition study of solids is one of the most common and widely used techniques to obtain insight into the elementary steps of solid-state reactions. Information on the kinetics and mechanism of solid decomposition is of both practical and theoretical importance [1,2]. Reactivity of solids is greatly modified by pre-treatments such as doping, pre-compression, pre-heating, etc. The nature of influence of the pre-treatments provides valuable information on the elementary steps of solid-state reactions and thereby on the mechanism and control of solid-state reactions [3,4]. Kinetic study is one of the important applications of thermal analysis. Solid-state kinetic data are of practical interest for the large and growing number of technologically important processes. A number of reviews are available in the literature on these processes [5–12].

Several methods have been applied for kinetic studies of solid-state reactions. The methods of kinetic analysis can be classified based on experimental conditions selected and the mathematical analysis performed. Experimentally, either isothermal or non-isothermal methods are used. The isothermal methods are based on the initial assumption that a single conversion function and a single set of Arrhenius parameters, A and E, apply over the full range of the conversion. A major problem encountered in the kinetic analyses of isothermal decomposition is the effect of pre-heating, on the sample [13]. This problem has been solved to a large extent by fabricating a thermobalance, particularly for studying isothermal kinetics of solid-state reactions [14]. We have reported the effects of pre-treatments on the thermal reactivity of several high-energy solids such as halates and perhalates [14–21] that throw light on the mechanism of their decomposition and also of other solid-state reactions in general and more data of this kind are desirable.

Thermoanalytical studies showed that KIO_4 decomposes in two steps [23,24]. At about 570 K, KIO_4 decomposes with heat evolution to potassium iodate (KIO_3) and oxygen. The decomposition of KIO_3 to KI takes place in the range of 780–800 K. In the thermal decomposition of KIO_4 it has not been proved possible to identify the hexavalent iodine compound, K_2IO_4, analogous to the compounds, M_2IO_4, formed in the decomposition of lithium and sodium periodates. Our earlier investigations [14,17] showed that the isothermal decomposition of KIO_4 proceeds through two stages, an acceleratory stage ($\alpha = 0.05$–0.5) and a decay stage ($\alpha = 0.5$–0.95), the former following the Prout–Tompkins kinetics and the latter contracting area kinetics, at all temperatures studied. These results prompted us to propose that the probable rate determining step in the thermal decomposition of KIO_4 is the transfer of an electron from the periodate anion to the potassium cation rather than the rupture of I–O bond or the diffusion of cations/anions

The studies on the effect of metal oxide additives (viz., CuO, MnO_2 and TiO_2) on the thermal decomposition kinetics of KIO_4 to potassium iodate (KIO_3) in air by thermogravimetry under isother-

---

* Corresponding author. Tel.: +91 494 2401144x413; fax: +91 4942400269.
E-mail address: kmuralika@gmail.com (K. Muraleedharan).

0040-6031/$ – see front matter © 2010 Elsevier B.V. All rights reserved.
doi:10.1016/j.tca.2010.01.025

mal conditions [21] revealed that irrespective of whether p- or n-type, the metal oxides show only a little or no influence on the rate of the decomposition except for the small decrease observed when the oxide concentration is as high as 10 wt%. This suggests that the electron work functions of these oxides might be smaller than that of KIO_4 so that they lack electron acceptor property with respect to KIO_4 and thus fail to favour electron-transfer processes. The rate laws for the decomposition of KIO_4 also remained unaffected by the additives. Studies on the effect of pre-compression, annealing and particle size on the isothermal decomposition kinetics of KIO_4 to KIO_3 have been investigated by thermogravimetry [22]. Although the effect of pre-compression was negligible up to an applied pressure of 5×10^3 kg cm^{-2}, the rate increased drastically on a further increase in pressure. Results of annealing indicate that gross imperfections are not easily annealed like point defects. Studies on the effect of particle size emphasize the need for fixing the particle size to enable a meaningful interpretation of the effects of pre-treatment on solid-state reactions. We observed that the rate law for the isothermal decomposition of KIO_4 remained unaffected by pre-treatments.

In continuation of our investigations on the thermal behaviour of periodates of alkali metals [14,17,20–22], in this paper we report the effect of the anion dopant phosphate and the cation dopant aluminium on the isothermal decomposition kinetics of KIO_4 in the temperature range of 560–580 K.

2. Experimental

All the chemicals used were of AnalaR grade from E Merck. Doped samples of KIO_4, at four concentrations, viz., 10^{-4}, 10^{-3}, 10^{-2} and 10^{-1} mol% were prepared by the method described earlier [14,17]. K_3PO_4 and $AlCl_3{\cdot}6H_2O$ were used for doping $PO_4{}^{3-}$ and Al^{3+}, respectively. The thermogravimetric (TG) measurements in static air were carried out on a custom-made thermobalance, fabricated in this laboratory [14], an upgraded version of Hooley [25].

A major problem [13] of the isothermal experiment is that a sample requires some time to reach the experimental temperature. During this period of non-isothermal heating, the sample undergoes some transformations that are likely to affect the succeeding kinetics. The situation is especially aggravated by the fact that under isothermal conditions, a typical solid-state process has its maximum reaction rate at the beginning of the transformation. So we fabricated a thermobalance particularly for isothermal studies, in which loading of the sample is possible at any time after the furnace attaining the desired reaction temperature. The operational characteristics of the thermobalance are balance sensitivity: $\pm 1 \times 10^{-5}$ g, temperature accuracy: ±0.5 K, sample mass: 5×10^{-2} g, particle size: 90–106 μm and crucible: platinum. Comparative runs were always made using samples of same age and particle size. The fraction of solid decomposed (α) was measured as a function of time (t) at five different temperatures (T), viz., 560, 565, 570, 575 and 580 K.

3. Results and discussion

The α–t curves for the decomposition of pure KIO_4 and the results of its thermal decomposition kinetics were reported earlier [14,17]. Similar curves were obtained for all doped samples of KIO_4 at all temperatures. The α–t curves for the decomposition of phosphate and aluminium doped KIO_4 at 570 K are respectively shown in Figs. 1 and 2. The decomposition proceeds mainly through two stages: (i) an acceleratory stage (α, 0.05–0.50) and (ii) the decay stage (α, 0.5–0.95).

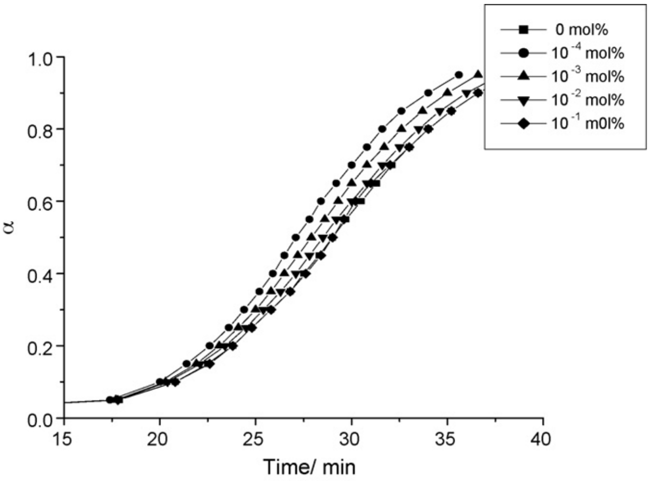

Fig. 1. α–t curves for the decomposition of pure and Al^{3+} doped KIO_4 at 570 K.

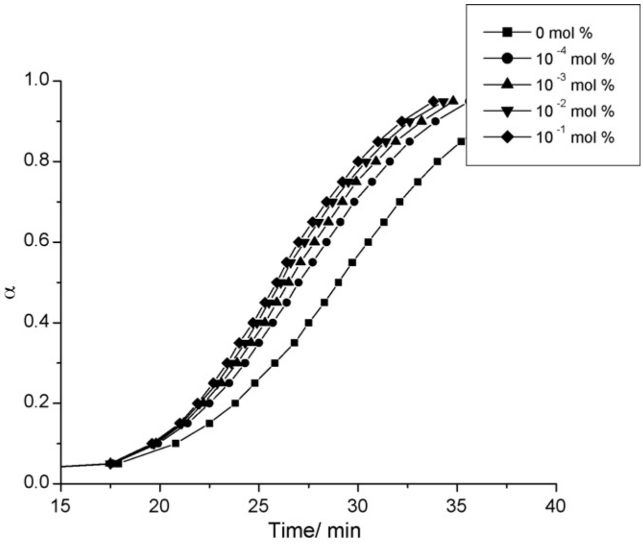

Fig. 2. α–t curves for the decomposition of pure and $PO_4{}^{3-}$ doped KIO_4 at 570 K.

The α–t data in the range of $\alpha = 0.05$–0.95 (range I) were fitted to various solid-state kinetic equations given in Table 1, using the method of weighted least squares as described earlier [17]. The Prout–Tompkins equation [26], $\ln[\alpha/(1-\alpha)] = kt$, which is the simplest case of an autocatalytic reaction, gave the best fits for the whole range of data at all the temperature studied. Separate kinetic

Table 1
Different reaction models used to describe the reaction kinetics.

SI. no.	Reaction model	Function $g(\alpha)$
1	Power law	$\alpha^{1/4}$
2	Power law	$\alpha^{1/3}$
3	Power law	$\alpha^{1/2}$
4	Power law	$\alpha^{3/2}$
5	One-dimensional diffusion	α^2
6	Mampel (first order)	$-\ln(1-\alpha)$
7	Avrami–Erofeev	$[-\ln(1-\alpha)]^{1/4}$
8	Avrami–Erofeyev	$[-\ln(1-\alpha)]^{1/3}$
9	Avrami–Erofeev	$[-\ln(1-\alpha)]^{1/2}$
10	Three-dimensional diffusion	$[1-(1-\alpha)^{1/3}]^2$
11	Contracting sphere	$1-(1-\alpha)^{1/3}$
12	Contracting cylinder	$1-(1-\alpha)^{1/2}$
13	Second order	$(1-\alpha)^{-1}-1$
14	Prout–Tompkins	$\ln[\alpha/(1-\alpha)]$

Table 2
Values of rate constants (k) for the decomposition of pure and aluminium doped KIO_4.

Temperature (K)	Dopant concentration (mol%)	k ($\times 10^3$ s^{-1})		
		Range I ($\alpha = 0.05$–0.95)	Range II ($\alpha = 0.05$–0.5)	Range III ($\alpha = 0.5$–0.95)
560	0	2.0294	1.8726	0.4221
	1×10^{-4}	2.2999	2.1333	0.4721
	1×10^{-3}	2.1592	2.0371	0.4394
	1×10^{-2}	2.0583	1.9248	0.4272
	1×10^{-1}	2.0554	1.9105	0.4259
565	0	2.9309	2.7498	0.6058
	1×10^{-4}	3.2964	3.1844	0.6339
	1×10^{-3}	3.1738	2.9945	0.6373
	1×10^{-2}	3.0268	2.7851	0.6216
	1×10^{-1}	2.9321	2.7528	0.6022
570	0	4.5308	4.4097	0.8609
	1×10^{-4}	5.1438	5.0829	0.9536
	1×10^{-3}	4.8846	4.8189	0.9225
	1×10^{-2}	4.6054	4.5152	0.8690
	1×10^{-1}	4.5962	4.3792	0.8478
575	0	6.6256	6.5701	1.2026
	1×10^{-4}	7.4074	7.0273	1.4511
	1×10^{-3}	6.8981	6.7762	1.3322
	1×10^{-2}	6.6204	6.5825	1.2273
	1×10^{-1}	6.9594	6.5667	1.2046
580	0	9.3259	9.3822	1.6968
	1×10^{-4}	11.4298	10.9499	2.3159
	1×10^{-3}	10.6373	10.5121	1.9526
	1×10^{-2}	9.8371	9.9859	1.8302
	1×10^{-1}	9.4622	9.6629	1.6484

analysis of the α–t data corresponding to the acceleratory region (range II) and decay region (range III) showed that the acceleratory stage gave the best fits with Prout–Tompkins equation [26] itself whereas the decay stage fitted better to the contracting area equation [27].

Doping with phosphate and aluminium did not change the basic shape (sigmoid) of the α–t plots and the decomposition proceeded through the same two stages obeying the same two rate laws mentioned above in the case of pure KIO_4. The values of rate constant (k) at various temperatures for different ranges of the decomposition of pure and doped samples of KIO_4 are given in Tables 2 and 3. The results show that the anion dopant phosphate enhances the rate of decomposition. The cation dopant aluminium behaves differently from the anion dopant in that the rate passes through a maximum as the concentration increases. Fig. 2 illuminates these effects.

Table 3
Values of rate constants (k) for the decomposition of pure and phosphate doped KIO_4.

Temperature (K)	Dopant concentration (mol%)	k ($\times 10^3$ s^{-1})		
		Range I ($\alpha = 0.05$–0.95)	Range II ($\alpha = 0.05$–0.5)	Range III ($\alpha = 0.5$–0.95)
560	0	2.0294	1.8726	0.4221
	1×10^{-4}	2.3001	2.1290	0.4754
	1×10^{-3}	2.3923	2.2620	0.4838
	1×10^{-2}	2.5132	2.4103	0.5012
	1×10^{-1}	2.5546	2.4605	0.5018
565	0	2.9309	2.7498	0.6058
	1×10^{-4}	3.3069	3.1660	0.6420
	1×10^{-3}	3.4056	3.3487	0.6490
	1×10^{-2}	3.5312	3.5246	0.6582
	1×10^{-1}	3.6185	3.6416	0.6645
570	0	4.5308	4.4097	0.8609
	1×10^{-4}	5.1335	5.1568	0.9484
	1×10^{-3}	5.3890	5.4120	0.9827
	1×10^{-2}	5.6072	5.7219	0.9942
	1×10^{-1}	5.7427	5.8310	1.0314
575	0	6.6256	6.5701	1.2026
	1×10^{-4}	7.4008	7.1754	1.4002
	1×10^{-3}	7.5611	7.5213	1.4524
	1×10^{-2}	7.9189	7.9255	1.4485
	1×10^{-1}	8.1600	8.2061	1.4842
580	0	9.3259	9.3822	1.6968
	1×10^{-4}	11.3560	10.7730	2.3343
	1×10^{-3}	12.0740	11.4190	2.3640
	1×10^{-2}	12.4590	11.8300	2.4794
	1×10^{-1}	12.9270	12.4970	2.5073

Table 4
Values of Arrhenious parameters for pure, phosphate and aluminium doped KIO_4.

Dopant	Dopant concentration (mol%)	Range[a]	E (kJ mol^{-1})	ln A (s^{-1})
Nil	0	I	209.01	38.69
		II	221.35	41.26
		III	187.54	32.51
Phosphate	1×10^{-4}	I	216.16	40.33
		II	219.59	41.01
		III	219.99	38.24
	1×10^{-3}	I	218.72	40.92
		II	218.80	40.90
		III	214.99	38.46
	1×10^{-2}	I	216.71	40.52
		II	215.83	40.33
		III	215.28	38.56
	1×10^{-1}	I	219.22	41.08
		II	219.64	41.17
		III	217.13	38.97
Aluminium	1×10^{-4}	I	217.08	40.53
		II	219.64	41.02
		III	216.54	38.78
	1×10^{-3}	I	214.36	39.89
		II	221.56	41.02
		III	200.72	35.37
	1×10^{-2}	I	211.44	39.22
		II	224.49	41.94
		III	194.03	33.91
	1×10^{-1}	I	211.85	39.31
		II	222.15	41.43
		III	183.82	31.72

[a] I: $\alpha = 0.05$–0.95; II: $\alpha = 0.05$–0.5; III: $\alpha = 0.5$–0.95.

The values of activation energy (E), and pre-exponentional factor (A) calculated from the rate constant–temperature data for pure and doped samples (Tables 2 and 3) are given in Table 4. We note that none of these dopants alters the activation energy of the decomposition process.

Philips and Taylor [28] proposed that the rupture of I–O bond determines the rate of the decomposition of KIO_4 to KIO_3. Contrary to the observation of Hill [29], they pointed out that the autocatalytic stage does not involve a diffusion chain and reported an apparent activation energy (E) value of 191 kJ mol^{-1} for the decomposition of KIO_4. Our earlier investigations [14,17] showed that the overall isothermal decomposition of KIO_4 follows Prout–Tompkins kinetics at all temperatures studied with an E value of 209 kJ mol^{-1}. The acceleratory stage was best described by Prout–Tompkins equation itself with an E value of 221 kJ mol^{-1}. However, the decay stage was best represented by the contracting area equation with an E value of 188 kJ mol^{-1}. Based on these results we suggested that KIO_4 decomposes in accordance with Prout–Tompkins model with two-dimensional nucleus growth up to 50% decomposition, and there after through contracting area law. Several authors [20,28,30–33] have reported such a description of reaction kinetics for the same solid using different rate laws for different ranges of α. Kim et al. [34] has reported that the reaction model varies with reaction temperature in isothermal pyrolysis of polypropylene and they observed that the Arrhenius parameters derived from the assumptions of nth order model would be improper.

The α–t data, in the range of $\alpha = 0.05$–0.95, of pure and doped (with phosphate and aluminium) KIO_4 were also subjected to isoconversional studies for the determination of apparent activation energy as a function of α from the sets of isothermals obtained. A plot of ln t (t being the time required for reaching a given value of α at a constant temperature T) versus the corresponding reciprocal of the temperature ($1/T$) would lead to the activation energy for the given value of α. The results are given in Table 5. A perusal of Table 5 reveals that the activation energy values for all samples in the range of $\alpha = 0.05$–0.95 lies in the range of 203–210 kJ mol^{-1}, which is in good agreement with those obtained from conventional method.

The rate laws and the activation energies of the isothermal decomposition of KIO_4 remain unaltered by doping. This suggests that the basic mechanism of the decomposition is not affected by doping, the only effect being a modification in the concentration of active sites.

Philips and Taylor [28] suggested a bond-breaking mechanism for the isothermal decomposition of KIO_4 based on the close agreement between the dissociation energy of I–O bond and the experimental activation energy. The cation and anion vacancies and in Frenkel systems the associated interstitial ions and also the lattice impurities alter the frequency of the lattice vibrations in the region surrounding the defect centers [32]. This contributes

Table 5
Activation energy values obtained from isoconversional method for pure and doped (with PO_4^{3-} and Al^{3+}) KIO_4.

α	E (kJ mol^{-1})								
	Pure KIO_4	PO_4^{3-} doped KIO_4				Al^{3+} doped KIO_4			
		10^{-4} mol%	10^{-4} mol%	10^{-4} mol%	10^{-4} mol%	10^{-4} mol%	10^{-4} mol%	10^{-4} mol%	10^{-4} mol%
0.05	203.05	202.62	202.62	203.77	203.30	202.59	202.81	202.86	204.09
0.10	206.09	205.03	204.31	206.06	204.67	204.12	204.32	205.00	206.38
0.15	205.81	205.71	205.95	205.71	205.80	205.61	205.24	203.57	205.89
0.20	206.75	206.46	206.53	206.51	206.08	205.74	205.87	205.98	205.75
0.25	207.88	206.44	206.76	206.58	206.57	205.37	206.02	206.66	206.16
0.30	208.96	207.38	207.31	207.13	207.88	207.10	206.68	207.60	207.23
0.35	208.54	207.50	207.29	207.36	207.52	207.64	206.22	207.49	207.74
0.40	208.53	208.38	207.37	207.44	207.72	207.89	207.65	207.90	207.92
0.45	209.72	208.34	208.06	207.64	207.91	207.69	208.20	209.76	208.72
0.50	209.71	208.29	208.42	207.88	208.38	207.87	208.67	209.50	209.76
0.55	209.85	208.16	208.91	208.28	208.65	207.70	208.59	208.94	209.76
0.60	209.26	208.42	208.78	208.38	208.74	207.94	208.47	208.10	209.76
0.65	208.45	208.79	208.92	208.75	209.11	208.06	208.07	207.46	209.76
0.70	208.13	208.58	208.92	208.91	209.10	208.18	207.55	206.75	209.76
0.75	207.39	208.55	209.50	208.75	209.53	208.92	207.35	207.11	209.76
0.80	206.33	208.88	209.31	208.63	209.38	209.38	207.56	207.04	209.76
0.85	206.33	208.94	209.25	208.93	209.36	208.94	207.47	207.25	209.76
0.90	205.63	209.21	209.61	209.06	209.22	209.58	207.54	206.71	209.76
0.95	204.67	209.54	209.93	210.08	210.46	208.19	207.11	206.30	209.76

substantially in weakening the chemical bonds in the vicinity of the defects and thus increases the reactivity of the solid. Therefore, on doping KIO_4 with either cation or anion will result in an increase in the rate of thermal decomposition if the rupture of I–O bond determines the rate. PO_4^{3-} and Al^{3+} doped KIO_4 samples do show an enhanced rate of decomposition, but only up to a dopant concentration of 10^{-4} mol% in the case of Al^{3+} (Fig. 1). At higher concentrations of Al^{3+}, however, the rate decreases without a change in the activation energy, which suggests the operation of the same mechanism in the low as well as high dopant concentration ranges. This fact can not be easily explained in terms of the bond-breaking mechanism, on the other hand, an electron-transfer mechanism proposed earlier [14] may be a suitable alternative.

The electron-transfer mechanism may be represented as follows:

$$K^+IO_4^- \rightarrow K^\bullet + IO_4^\bullet \quad (1)$$

$$IO_4^\bullet \rightarrow IO_3^\bullet + O^\bullet \quad (2)$$

$$O^\bullet + O^\bullet \rightarrow O_2 \quad (3)$$

$$K^\bullet + IO_3^\bullet \rightarrow KIO_3 \quad (4)$$

Step (1) involves the transfer on an electron from the periodate anion to potassium cation to form the free radicals $K^\bullet$ and $IO_4^\bullet$. As $IO_4^\bullet$ involves a one-electron bond, it is very unstable and readily decomposes to give $O^\bullet$ and relatively stable $IO_3^\bullet$ [step (2)]. Two $O^\bullet$ species combine to give one oxygen molecule [step (3)]. In step (4), $IO_3^\bullet$ is stabilized by receiving an electron from $K^\bullet$ forming KIO_3. In the above scheme steps (2)–(4) are fast since they involve highly reactive species. The electron-transfer processes, step (1), is the slowest and plays an important role in determining the rate. The present results support this mechanism as can be seen below.

Doping KIO_4 with phosphate introduces additional anion vacancies in the solid. Anion vacancies can capture electrons and thus function as electron traps (T) because of the localization of positive charge in their neighborhood [7,27]. An anion vacancy traps an electron from the neighboring periodate anion to produce $IO_4^\bullet$ which decomposes to $IO_3^\bullet$ and $O^\bullet$. The trapped electron is then transferred to K^+ to produce, $K^\bullet$, which combines with $IO_3^\bullet$ to form KIO_3:

$$IO_4^- + T \rightarrow IO_4^\bullet + Te \quad (5)$$

$$IO_4^\bullet \rightarrow IO_3^\bullet + O^\bullet \quad (6)$$

$$Te + K^+ \rightarrow K^\bullet + T \quad (7)$$

Thus the anion vacancy acts as a bridge between the periodate anion and potassium cation facilitating the electron transfer. When concentration of the dopant ion increases the number of anion vacancies (i.e., T) also increases. Consequently the rate of formation and growth of nuclei is promoted resulting in an enhanced rate of decomposition in proportion to the dopant level. Being triply charged, each phosphate ion added to KIO_4 will generate two anion vacancies. Justifying this, here we observed a higher rate of decomposition than that with sulphate doped KIO_4.

Incorporation of Al^{3+} into KIO_4 lattice generates cation vacancies and this result in a decrease in the number of anion vacancies. Thus, in the event of the validity of electron-transfer mechanism, one would expect a continuous decrease in the rate on doping KIO_4 with Al^{3+}. But the rate of decomposition shows a complex dependence on dopant concentration; the rate first increases reaching a maximum value at around 10^{-4} mol% and then falls on further increase in the dopant level (Fig. 2). Similar results were obtained for Ba^{2+} doped KIO_4 [19]. Now considering the polarizing power of a cation, which is proportional to Ze/R^2, where Z is its valance, R its radius and e the electronic charge, the kinetic results obtained for doped KIO_4 cam be interpreted as follows. The high Z and small R values make the polarizing power of Al^{3+} very high. As anions are readily polarizable due to the diminished control of electron cloud by the nucleus, it is easy for Al^{3+} to strongly polarize the diffused electron cloud of the periodate anion and even capture an electron from it. In other words, Al^{3+} itself acts as an electron trap and promotes the decomposition according to the above scheme [steps (5)–(7)] where T stands for Al^{3+} and Te for Al^{2+}. Thus doping with Al^{3+} results in two concurrent effects, having opposite influence on rate: (i) enhancement of electron-transfer rate by the action of Al^{3+}, as electron traps and (ii) suppression of the rate due to a decrease in the number of anion vacancies which are good electron traps. The results suggest that the enhancing effect predominates at low concentrations of Al^{3+}, whereas suppression takes upper hand at high concentrations possibly because of the association of the positively charged Al^{3+} with negatively charged cation vacancies (+) and the consequent lowering of the concentration of impurity ions acting as an electron traps. The situation may be represented as:

$$Al^{3+} + 2(+) \rightarrow \{(+)Al^{3+}(+)\} \quad (8)$$

With respect to the occupancy of lattice sites, Al^{3+} has a charge of +2 and (+) has −1; hence the assembly {(+) Al^{3+} (+)} is neutral. The dopant Al^{3+} is thus rendered ineffective as electron trap by the association of the defects and consequently the inhibiting effect (due to the decrease in the concentration of anion vacancies) predominates. This type of electrostatic interaction of defects is more probable at high concentration of Al^{3+} and cation vacancies due to the high probability of occurrence of these defects in close proximity of each other within the solid. As a result the rate of decomposition decreases steadily as the concentration of Al^{3+} increases, as is observed in this investigation (Fig. 2). Similar results were obtained for Ba^{2+}, but the magnitude of the effect in rate was low as is to be expected from its lower polarizing power.

A similar association between PO_4^{3-} dopant and anion vacancies (−) is not possible because interstitial as well as vacancy diffusion of phosphate is unlikely due to its larger size. It may be further noted that, because of the better proximity, the interaction of a cation dopant occupying an interstitial site with a cation vacancy, is stronger than the interaction of an anion dopant occupying a normal site, with an anion vacancy. This means that deactivation of anion vacancies by their association with anion dopants is not significant in anion doped samples and therefore these samples show a normal increase in rate with dopant concentration.

4. Conclusions

The results favour an electron-transfer mechanism for the thermal decomposition of KIO_4 rather than a bond-breaking mechanism. Further the study demonstrates the extreme sensitivity of solids towards lattice impurities and emphasizes that extreme care should be taken in interpreting the effect of both cationic and anionic impurities for elucidating the mechanism of decomposition. A study using a wide range of concentration of the impurities is invariably required to unveil the actual mechanism.

Acknowledgement

The authors are thankful to KSCSTE for providing the financial assistance.

References

[1] A.K. Galwey, M.E. Brown, Thermal Decomposition of Ionic Solids, Elsevier, Amsterdam, 1999.

[2] S. Vyazovkin, Int. Rev. Phys. Chem. 19 (2000) 45–60.

[3] P.J. Herley, P.W.M. Jacobs, P.W. Levy, Proc. R. Soc. Lond. 318A (1970) 197–211.

[4] V.R. Pai Verneker, K. Rajeshwar, J. Phys. Chem. Solids 37 (1976) 63–66.

[5] V.A. Benderskii, D.E. Makarov, C.A. Wight, Chemical Dynamics at Low Temperatures, Wiley, New York, 1994, p. 385.
[6] M.E. Brown, D. Dollimore, A.K. Galwey, Reactions in the Solid State, Comprehensive Chemical Kinetics, vol. 22, Elsevier, Amsterdam, 1980, p. 340.
[7] T.B. Brill, K.J. James, Chem. Rev. 93 (1993) 2667–2692.
[8] J.H. Flynn, in: H.F. Mark, N.M. Bikales, C.G. Overberger, G. Menges (Eds.), Encyclopedia of Polymer Science and Engineering, Wiley, New York, 1989, p. 690.
[9] J. Sestak, Thermophysical Properties of Solids, Comprehensive Analytical Chemistry, vol. 12D, Elsevier, Amsterdam, 1984, p. 440.
[10] J.G. Fatou, in: H.F. Mark, N.M. Bikales, C.G. Overberger, G. Menges (Eds.), Encyclopedia of Polymer Science and Engineering, Wiley, New York, 1989, p. 231.
[11] A.K. Galwey, Thermochim. Acta 413 (2004) 139–183.
[12] D. Dollimore, Chem. Rev. 68 (1996) 63–72.
[13] S. Vyazovkin, C.A. Wight, Annu. Rev. Phys. Chem. 48 (1997) 125–149.
[14] K. Muraleedharan, M.P. Kannan, Thermochim. Acta 359 (2000) 161–168.
[15] M.P. Kannan, J. Thermal. Anal. 32 (1987) 1219–1227.
[16] K. Muraleedharan, M.P. Kannan, React. Kinet. Catal. Lett. 39 (2) (1989) 339–344.
[17] M.P. Kannan, K. Muraleedharan, Thermochim. Acta 158 (1990) 259–266.
[18] T. Gangadevi, M.P. Kannan, B. Hema, Thermochim. Acta 285 (1996) 269–276.
[19] M.P. Kannan, T. Gangadevi, Thermochim. Acta 292 (1997) 105–109.
[20] M.P. Kannan, V.M. Abdul Mujeeb, React. Kinet. Catal. Lett. 72 (2001) 245–252.
[21] K. Muraleedharan, M.P. Kannan, T. Gangadevi, J. Therm. Anal. Calorim. (2009), doi:10.1007/s10973-009-0411-y (published online on 29.08.2009).
[22] K. Muraleedharan, M.P. Kannan, T. Gangadevi, React. Kinet. Catal. Lett., Submitted for publication.
[23] O.N. Breusov, N.J. Kashina, T.V. Rezvina, Zh. Neorg. Khim 15 (1970) 612–614.
[24] P. Bianco, R. Subbah, G. Perinet, Bull. Soc. Chim. 9 (1967) 3437–3442.
[25] J.G. Hooley, Can. J. Chem. 35 (1957) 374–380.
[26] E.G. Prout, F.C. Tompkins, Trans. Faraday Soc. 40 (1944) 488–497.
[27] A.K. Galwey, Chemistry of Solids, Science, Paper Backs, 1967, p. 179.
[28] B.R. Philips, D. Taylor, J. Chem. Soc. (1963) 5583–5590.
[29] R.A.W. Hill, Trans. Faraday Soc. 54 (1958) 685–690.
[30] M.M. Markowitz, D.A. Boryta, J. Phys. Chem. 65 (1961) 1419–1424.
[31] K.H. Stern, High Temperature Properties and Thermal Decomposition of Inorganic Salts with Oxyanions, CRC Press, 2001, ISBN 0-8493-0256-0.
[32] A.K. Galwey, M.E. Brown, Thermal decomposition of ionic solids, in: Studies in Physical and Theoretical Chemistry, Elsevier Scientific, Amsterdam, 1999.
[33] F. Solymosi, Structure and Stability of Salts of Halogen Oxyacids in the Solid Phase, John Wiley & Sons, London, 1977.
[34] S. Kim, D. Kavitha, T.U. Yu, J.-S. Jung, J.-H. Song, S.-W. Lee, S.-H. Kong, J. Anal. Appl. Pyrolysis 81 (2008) 100–105.